Atmospheric
Chemistry
and Physics
Discussions

Open Access

Inconsistencies between chemistry climate model and observed lower stratospheric trends since 1998

William T. Ball[1,2], Gabriel Chiodo[1,3], Marta Abalos[4], and Justin Alsing[5,6]

[1]Institute for Atmospheric and Climate Science, Swiss Federal Institute of Technology Zurich, Universitaetstrasse 16, CHN, CH-8092 Zurich, Switzerland

[2]Physikalisch-Meteorologisches Observatorium Davos World Radiation Centre, Dorfstrasse 33, 7260 Davos Dorf, Switzerland

[3]Department of Applied Physics and Applied Mathematics, 5 Columbia University, New York, NY, USA

[4]Earth Physics and Astrophysics Dep., Universidad Complutense de Madrid, Avda. Complutense s/n, 28040 Madrid, Spain

[5]Oskar Klein Centre for Cosmoparticle Physics, Stockholm University, Stockholm SE-106 91, Sweden

[6]Imperial Centre for Inference and Cosmology, Department of Physics, Imperial College London, Blackett Laboratory, Prince Consort Road, London SW7 2AZ, UK

Correspondence to: W. T. Ball (william.ball@env.ethz.ch)

Abstract. The stratospheric ozone layer shields surface life from harmful ultraviolet radiation. Following the Montreal Protocol ban of long-lived ozone depleting substances (ODSs), rapid depletion of total column ozone (TCO) ceased in the late 1990s and ozone above 32 km now enjoys a clear recovery. However, there is still no confirmation of TCO recovery, and evidence has emerged that ongoing quasi-global (60°S–60°N) lower stratospheric ozone decreases may be responsible, dominated by low latitudes (30°S–30°N). Chemistry climate models (CCMs) used to project future changes predict that lower stratospheric ozone will decrease in the tropics by 2100, but not at mid-latitudes (30°–60°). Here, we show that CCMs display an ozone decline similar to that observed in the tropics over 1998–2016, likely driven by a increase of tropical upwelling. On the other hand, mid-latitude lower stratospheric ozone is observed to decrease, while CCMs show an increase. Despite opposing lower stratospheric ozone changes, which should induce opposite temperature trends, CCM and observed temperature trends agree; we demonstrate that opposing model-observation stratospheric water vapour (SWV) trends, and their associated radiative effects, explain why temperature changes agree in spite of opposing ozone trends. We provide new evidence that the observed mid-latitude trends can be explained by enhanced mixing between the tropics and extratropics. We further show that the temperature trends are consistent with the observed mid-latitude ozone decrease. Together, our results suggest that large scale circulation changes expected in the future from increased greenhouse gases (GHGs) may now already be underway, but that most CCMs are not simulating well mid-latitude ozone layer changes. The reason CCMs do not exhibit the observed changes urgently needs to be understood to improve confidence in future projections of the ozone layer.

1 Introduction

In the latter half of the 20$^{\text{th}}$ Century, emissions of halogen-containing ozone depleting substances (ODSs) led to a decline of the ozone layer at all latitudes across the globe (WMO, 2014). Following the almost universal implementation of the Montreal Protocol and its amendments (MPA) by governments, production of ODSs halted soon after and ODS loading in the atmosphere peaked in the mid-to-late 1990s (Newman et al., 2007; Chipperfield et al., 2017). By 1998, quasi-global (60°S–60°N) total column ozone had globally declined by ~5%, and spring-time ozone over the Antarctic regularly saw losses of two-thirds in the total column (WMO, 2018). In subsequent years, it emerged that global total column ozone levels had stopped falling by around 1998–2000 thanks to the MPA (WMO, 2006), and research has turned to identifying an ozone recovery related to ODS declines (Chipperfield et al., 2017). In the upper stratosphere (1–10 hPa; 32–48 km), ozone now enjoys a clear recovery with levels now significantly above those of 1998 (Bourassa et al., 2017; Sofieva et al., 2017; Steinbrecht et al., 2017; Ball et al., 2017; WMO, 2018; Petropavlovskikh et al., 2019). The area of the Antarctic ozone hole during September and October is now also showing signs of year-on-year shrinkage (Solomon et al., 2016; Pazmino et al., 2017; WMO, 2018). As such, there

are clear indications that the MPA has worked in reducing atmospheric ODSs, that further significant and serious depletion of the ozone layer has been avoided (Egorova et al., 2013; Chipperfield et al., 2015), and that some regions exhibit an MPA-dependent recovery.

However, the picture has become more complicated, particularly in the lower stratosphere. Recent
40   findings indicate that contrary to chemistry climate model (CCM) predictions, ozone in the lower stratosphere has continued to decrease over 1998-2016 (Ball et al., 2018; Zerefos et al., 2018; Wargan et al., 2018; Ball et al., in review, 2019) and is offsetting the increases in the upper stratosphere (Ball et al., 2018). Changes and variability related to dynamics have been proposed as a mechanism, with evidence from reanalysis data (Wargan et al., 2018) and a chemistry transport model (CTM)
45   (Chipperfield et al., 2018). Rising tropospheric ozone (Ziemke et al., 2018; Gaudel et al., 2018) also interferes in clearly detecting an ozone layer increase when considering total column ozone alone as a proxy for the ozone layer (Ball et al., 2018). A statistically significant increase in total column ozone since 1998 or 2000 remains undetected (Weber et al., 2018).

A confounding factor in detecting an ODS-related recovery is that rising greenhouse gas (GHG)
50   concentrations also affect the apparent recovery rate in the stratosphere through two main processes. Increased GHGs lead to a cooling of the stratosphere, thereby slowing temperature-dependent catalytic reaction rates that destroy ozone, and ~50% of the upper stratospheric ozone increase has been attributed to GHG-induced temperature decreases (WMO, 2014). Rising GHGs are also expected to modify the wave-driving of the large-scale Brewer-Dobson circulation (BDC) (see Butchart (2014)
55   and references therein), mainly through an acceleration of tropical upwelling that CCMs robustly simulate in projections towards the end of the 21st Century. This upwelling is correlated with a decline in tropical lower stratospheric ozone (SPARC/WMO, 2010) that means, by 2100, total column ozone in the tropics will not have recovered to pre-1980s levels (Eyring et al., 2010; Dhomse et al., 2018). However, it has not been demonstrated, using CCMs, that mid-latitude (30°–60°) lower strato-
60   spheric ozone should decrease and, indeed, multi-model mean (MMM) estimates that aggregate multiple CCMs indicate positive, though non-significant, changes at mid-latitudes by 2013 (WMO, 2014) or 2016 (WMO, 2018).

It has been proposed that the decline in ozone detected at mid-latitudes is a consequence of large natural variability interfering with linear regression trend analysis (Stone et al., 2018; Chipperfield
65   et al., 2018). A southern hemisphere (SH) increase in ozone in 2017 was simulated using a chemistry transport model (CTM) to exceed the estimated long-term decrease over the previous 19 years when integrated over the quasi-global lower stratosphere (Chipperfield et al., 2018). When observations became available this short-term, large increase in ozone was found to be ~60% of the modelled change (Ball et al., in review, 2019), and 2018 saw quasi-global ozone begin to decrease again
70   towards the end of the year; a seasonal dependence of the quasi-biennial oscillation (QBO) has been implicated as the primary driver of these mid-latitude changes, i.e. dynamically driven. Due to the absence of an interaction of seasonal and QBO terms in the regression analysis, such non-

Atmospheric
Chemistry
and Physics
Discussions
Open Access
EGU

linearities are not considered and the large dynamical changes are not accounted for, leading to large residuals that can indeed influence trend terms. In the particular case of 2017, while the magnitude

75   and probability of the inferred negative ozone change for 1998–2017 in the SH lower stratosphere have reduced relative to 1998–2016, it remains negative; equatorial and NH changes remain negative with similar confidence over the last few years.

The aforementioned CTM (Chipperfield et al., 2018) drives the dynamics, temperature and surface level pressure using reanalysis (Dee et al., 2011) – a coherent, historical assimilation of observations

80   using a general circulation model – that aims to reproduce historical behaviour of the atmosphere as closely as possible to compare with observations. The chemistry, however, is allowed to evolve freely and, generally, a CTM can simulate the observed behaviour of ozone reasonably well. It has also been shown that two state-of-the-art CCMs that use reanalyses in specified-dynamics (SD) mode – that is to guide, but not govern, the dynamics of models – do not reproduce the changes

85   seen in the lower stratosphere (Ball et al., 2018). This is despite the aim of such models to reproduce historical dynamical changes while allowing freedom for the models to evolve in their own, model-dependent way. Why they do not reproduce the observations remains an open question. At the other end of the model spectrum are free-running (FR) CCMs – with no interference from reanalyses in governing dynamics. FR CCMs are used to investigate how the atmosphere responds to different

90   forcing scenarios, and future projections of GHG and ODS changes (WMO, 2018); in this mode each model generates its own, model-dependent, internal variability. Apart from a direct comparison of MMM results with the observations (Steinbrecht et al., 2017; WMO, 2018; Petropavlovskikh et al., 2019), a comprehensive comparison of the observed changes in the lower stratosphere with observations on timescales from 1998 to present have not yet been performed, and is one of the goals

95   of this study.

From a modelling perspective, averaging multiple CCMs into a MMM suppresses unforced natural variability and therefore reduces uncertainties in trend analyses; it can also lead to a loss of information regarding the sensitivity of CCMs to a changing state, and the range of responses to drivers; warnings against such averaging to understand CCM efficacy have been raised before (Dou-

100   glass et al., 2012, 2014). Thus, considering the spread in single CCM realisations might provide insight on the probability of the mid-latitude trends occurring by chance, if one or some of the realisations can reproduce the mid-latitude declines. A study investigating the spread of stratospheric ozone trends in nine ensembles members of the WACCM CCM over 1998 to 2016 found trends ranging from ±6% in the lower stratosphere (Stone et al., 2018), a similar magnitude to those in

105   the observations, though the extremities of this range were only found over the equator, and none of these members showed the spatially-resolved, wide-spread (50°S–50°N) and coherent decreases found in the observations. Absence of coherence in WACCM in the aforementioned ensemble runs does not imply that natural variability is not interfering with trends, but an expansion of exploring this possibility to more models, as we will do here, is needed to build confidence in this argument.

110   Many past studies, and assessments, have usually considered changes in ozone from 1960 to 2100, sub-periods within, or MMM changes since 1998 and 2000 up to the time of the study (Eyring et al., 2010; SPARC/WMO, 2010; WMO, 2014; Dhomse et al., 2018; WMO, 2018). MMM changes in ozone already indicate that by 2013 (WMO, 2014) and 2016 (Petropavlovskikh et al., 2019), tropical ozone should exhibit negative trends and mid-latitudes positive trends, albeit insignificant in

115 both cases. The recent findings of decreasing lower stratospheric ozone across mid-latitudes and the tropics raises the question of whether any FR models among the MMM can reproduce these changes, and focuses a comparison of FR CCMs specifically over 1985–2016 (or similar periods) with which to compare with recent observational studies. This study will also consider this issue.

       We find that, to understand the differences (and agreement) between the observations and CCMs,

120 we need to look beyond ozone and determine if the signature of decreasing ozone is consistent with other variables, such as dynamical changes and temperature. More explicitly, the implication of increasing ozone at mid-latitudes in FR CCMs suggest that temperature, for which ozone is a primary driver in this region, might be increasing. Yet, a recent comparison of FR CCMs with improved lower stratospheric temperature observations showed temperatures have continued to decline in both

125 observations and FR CCMs (Maycock et al., 2018), albeit slower after 2000 than before; while CO_2 is responsible for ongoing temperature decreases in the upper stratosphere, it has little influence in the lower stratosphere (Brasseur and Solomon, 2005). As such, the agreement leads to a paradox with respect to ozone and temperature at mid-latitudes that we also resolve here by considering trends in stratospheric water vapour (SWV), which is also an important driver of trends in the lower

130 stratosphere.

       In the following, we first lay-out the suite of ozone, temperature, and SWV observations, reanalyses products for estimates of dynamical changes (section 2.1), and the CCMs we consider (section 2.2). We use dynamical linear modelling (DLM) to estimate long-term changes, and how they evolve, and fixed dynamical heating (FDH) calculations to quantify temperature changes induced by

135 changes in ozone and SWV; these methods are laid out in sections 2.3 and 2.5, respectively. Following that, we begin by presenting results of changes since 1998 comparing ozone observations with CCMs, in different regions of the lower stratosphere (section 3.1). We use dynamical changes from reanalysis to understand why ozone is decreasing in the tropics and mid-latitudes (section 3.2). Given the paradox of temperature and ozone changes (section 3.3), we then turn to SWV changes

140 and FDH calculations to resolve the temperature changes (section 3.4). We bring together all of these results in the discussion (section 3.5), and then conclude (section 4).

2 Data and methods

2.1 Observations and reanalyses

For the resolved stratosphere and partial column ozone (PCO), we use the BASIC$_{SG}$ composite
145 as used in Ball et al. (2018) – data are found at https://data.mendeley.com/datasets/2mgx2xzzpk/2
(Alsing and Ball, 2017). This composite merges SWOOSH (Davis et al., 2016) and GOZCARDS
(Froidevaux et al., 2015, 2019) ozone composites using the BASIC approach (Ball et al., 2017);
BASIC uses information in both composites to remove artefacts, including jumps and drifts (see
examples in Supplementary Materials of Ball et al. (2018)).

150 For total column ozone, we use SBUV MOD v8.6 (Frith et al., 2014) which shows good agreement
with other TCO composites (Chehade et al., 2014; Weber et al., 2018).

Long-term stratospheric temperature observations are limited to a few stratospheric levels, with
particularly low vertical resolution in the lower stratosphere. We use NOAA microwave sounding
unit-4 (MSU4) for observations of lower stratospheric temperature; this has a large vertical kernel
155 that peaks at approximately 80 hPa (∼18 km) but reaches down to 300 (8-15 km) and up to 20 hPa
(∼27 km), though the bulk of the kernel is in the stratosphere, roughly between 50 and 150 hPa
(Penckwitt et al., 2015).

Stratospheric water vapour (SWV) observational changes are estimated from the filled SWV prod-
uct of SWOOSH (Davis et al., 2016).

160 We use the Japanese 55-year reanalysis (JRA-55) (Ebita et al., 2011; Kobayashi et al., 2015)
and the Interim European Centre for Medium-Range Weather reanalysis (ERA-Interim) Dee et al.
(2011) fields to investigate residual circulation upwelling (w*) and mixing efficiency, estimated as the
effective diffusivity computed from potential vorticity (Abalos et al., 2016; Haynes and Shuckburgh,
2000)

165 2.2 CCMVal-2 models

We use the REF-B2 CCM simulations from the chemistry climate model validation (CCMVal-2)
(SPARC/WMO, 2010; Eyring et al., 2010) as used in the WMO 2014 ozone assessment report to
compare with observations. REF-B2 are simulations to 2100 with future scenarios ODS (adjusted
Scenario A1) and GHG (SRES-A1b) boundary conditions (SPARC/WMO, 2010) and although so-
170 lar cycle, prescribed QBO, or volcanic aerosols should be included, they are not necessarily in ev-
ery case. Sea surface temperature (SST) and sea ice cover (SIC) are provided as boundary condi-
tions from simulations of other climate models such that, e.g., ENSO is not similar to historical
behaviour. As such, we did not include the aforementioned regressors in the DLM analysis, meaning
for CCMVal-2 models, we only derive seasonal cycle and non-linear trends, while for the observa-
175 tions we do (see DLM section 2.3).

We used results from 12 CCMVal-2 models (and a total of 21 ensemble members) as follows. Ensemble means are estimated where more than one existed (number of ensembles in brackets): CAM3.5 (1), CCSRNIES (1), CMAM (3), CNRM-ACM (1), LMDZ (1), MRI (2), Niwa-SOCOL (1), SOCOLv3 (3), ULAQ (3), UMSLIMCAT (1), UMUKCA-UCAM (1), and WACCM-CESM (3). We calculated two multi model means (MMMs) including all models (MMM-Am), and a sensitivity including the first ensemble of each (MMM-1m); the results changed little. We also checked the sensitivity of the results by excluding CAM3.5 since results in the upper stratosphere (above 20 hPa) are not available; Fig. S5a shows virtually no affect on the middle and lower stratospheric ozone changes. Further, we performed another sensitivity test to see how removal of several CCMs would impact the lower stratosphere, which were chosen due to specific features of the run or output that made testing the impact of their removal on the MMM worth checking. These models were: CAM3.5 (missing results in the upper stratosphere), UMUKCA-UCAM (climatological SWV), UMSLIMCAT (no SWV available), and CNRM-ACM (no SWV available); again the results remained similar, so we do not remove them for the full analysis performed in the paper. As no SWV is available for CNRM-ACM and UMSLIMCAT, these are absent in the SWV MMMs and SWV 1998–2016 changes. UMUKCA-UCAM SWV is climatological and displays no change. Analysis of multi-model means (MMMs) were performed by averaging original model outputs and then performing the DLM analysis.

2.3 Regression analysis with dynamical linear modelling (DLM)

Regression analysis is performed using DLM (Alsing, 2019) following Ball et al. (2017, 2018, in review, 2019). Similar to ordinary least squares multiple linear regression (MLR; e.g. WMO (2006, 2014); Harris et al. (2015); Steinbrecht et al. (2017); Ball et al. (2017)) a set of regressors (predictor variables) are used to represent known variability: the 30 cm solar radio flux (F30) (Dudok de Wit et al., 2014), a latitude-dependent stratospheric aerosol optical depth (SAOD; (Thomason et al., 2017)), the NOAA El Nino Southern Oscillation (ENSO) 3.4 index (from NOAA: http://www.esrl.noaa.gov/psd/enso/mei/table.html), two Quasi-Biennial Oscillation (QBO) proxies at 30 and 50 hPa from the Freie Universitaet (http://www.geo.fu-berlin.de/en/met/ag/strat/produkte/qbo/index.html), the Arctic and Antarctic Oscillation, AO/AAO (http://www.cpc.ncep.noaa.gov/products/precip/CWlink/), as proxies for Northern and Southern surface pressure variability, and an auto-regressive (AR1) process (Tiao et al., 1990). In contrast to MLR, the main advantage of DLM is the non-linear trend and evolving seasonal cycle. For the seasonal cycle, DLM estimates 6- and 12- month harmonics for the seasonal cycle at the same time as the other regressor amplitudes. Additionally, the trend is not predetermined with a linear or piece-wise linear model, but is allowed to slowly vary and the degree of trend non-linearity is an additional free parameter that is jointly inferred from the data along with the trend, seasonal cycle and regressor amplitudes, and AR process; see Laine et al. (2014)] and Ball et al. (in review, 2019) for more details.

2.4 Statistics

We infer posterior distributions on the non-linear trends by Markov Chain Monte Carlo (MCMC) sampling using the public code DLMMC (Alsing, 2019). DLM analyses like the one performed here typically have more conservative uncertainties on the trend than MLR since DLM represents a more flexible regression model, and (in this case) formally marginalizes over uncertainties in the regression coefficients, seasonal cycle, autoregressive process and coefficients, and parameters characterizing the degree of non-linearity in the trend (Ball et al., in review, 2019). Probabilities of changes are estimated from the sampled posterior distributions; we apply Gaussian kernel-density estimates (KDEs) to the MCMC samples to estimate the marginal posterior probability density functions (PDFs), and probabilities of a change quoted in the manuscript are estimated from integrals of these PDFs.

2.5 Fixed dynamical heating (FDH) calculations

We use the Parallel Offline Radiative Transfer (PORT) model (Conley et al., 2013) to quantify the (radiative) contribution of ozone and SWV to temperature changes in the stratosphere in models and observations. This is done by imposing ozone and SWV perturbations in PORT, and allowing the stratosphere to radiatively adjust in offline calculations, while keeping dynamical heating and tropospheric temperatures fixed: this is the so-called Fixed Dynamical Heating (FDH) approximation, a method commonly used to compute the stratosphere-adjusted radiative forcing (e.g. Fels et al. (1980)). Following the approach of previous work (Forster and Shine, 1997), we consider the temperature adjustment above the tropopause layer that is required for the stratosphere to reach radiative equilibrium, as the contribution of each of the species to the trends.

3 Results

3.1 Ozone: observed mid-latitude lower stratospheric trends do not match modelled changes

The successful implementation of the Montreal Protocol led to TCO depletion halting in ~2000, but no significant increase has yet been observed (Fig. 1a) (Weber et al., 2018; Chipperfield et al., 2018; WMO, 2018). The MMM of 12 CCMs from the Chemistry Climate Model Validation phase 2 (CCMVal-2) (SPARC/WMO, 2010; WMO, 2014; Dhomse et al., 2018) indicates a significant recovery should be underway (Fig. 1b); all individual CCMs, except one, reflect this behaviour in TCO (see supplementary materials Fig. S1a). The 60°S–60°N ozone layer is observed to have likely continued to thin due to lower stratospheric ozone decreases (Fig. 1a) that counteract an upper stratospheric recovery (Ball et al., 2018), which are not reproduced by the MMM (Fig. 1b). While lower stratospheric ozone (Fig. 1a) exhibits a monotonic decline in contrast to the behaviour of TCO, the trends are qualitatively similar in their second derivative (acceleration; Fig. 1c), with a slower
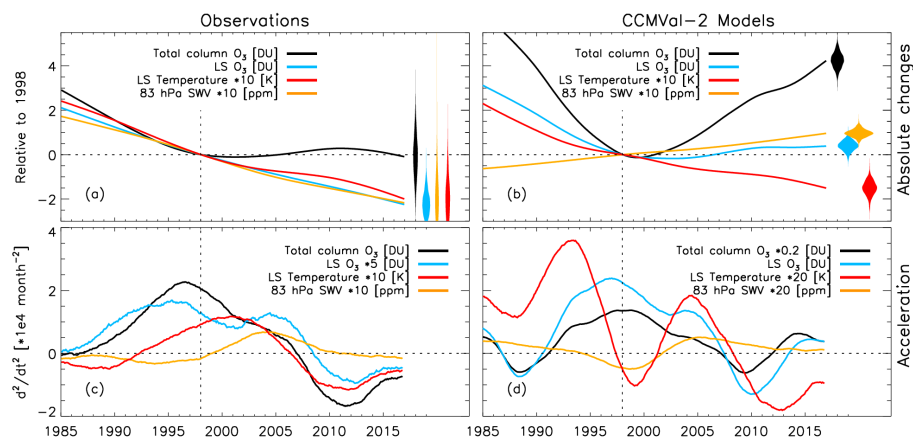
Figure 1: Global 60°S–60°N 1985–2016 stratospheric changes. **(a)** Observed non-linear trends for total column ozone (black), lower stratospheric ozone (blue), temperature (red) and stratospheric water vapour (SWV, yellow) relative to 1998, and their respective **(c)** acceleration curves (5–year smoothing); **(b,d)** as for (a,c) but for the multi-model mean (MMM). Units and scaling of each variable are indicated in the legends.

post-1997 decline that accelerates after 2009, and similar inflection times after 2000. This correlated behaviour can be explained by the large contribution of the lower stratosphere to the TCO. The same qualitative similarities in TCO and lower stratospheric ozone trends is seen for the MMM, but with acceleration five-times larger compared to the observations (Fig. 1d). Nevertheless, observation-model lower stratospheric ozone changes disagree significantly (Fig. 1a,b) and drive much of the TCO observation-MMM difference, although it should be noted that uncertainty remains in changes within the tropospheric component of TCO (Ball et al., 2018; Gaudel et al., 2018; Ziemke et al., 2018). We note that the 50°–60° region in both hemispheres shows relatively flat lower stratospheric ozone trends (Ball et al., in review, 2019), and therefore the quasi-global integrated changes are driven by the 50°S–50°N region (see similar results in Figs. S1–S3); we therefore focus on this region.

Figure 2a–c shows the observed, CCM ensemble and MMM changes in lower stratospheric ozone from 1998–2016, in three sub-regions: southern hemisphere mid-latitudes (SH, 50°–30°S), the tropics (20°S–20°N), and northern hemisphere mid-latitudes (NH; 30°–50°N). Total column ozone (Fig. S2) and quasi-global (60°S–60°N, Fig. S1; 50°S–50°N, Fig. S3) changes are provided in the supplementary materials. A MMM sensitivity test that considers only one-ensemble member of each model (MMM-1m) to avoid biasing the MMM to models with more members, shows little difference to including all (MMM-Am). Over the tropics (Fig. 2b), both the MMM and observations indicate a significant decrease and, while some CCMs agree in the magnitude, observations show a stronger
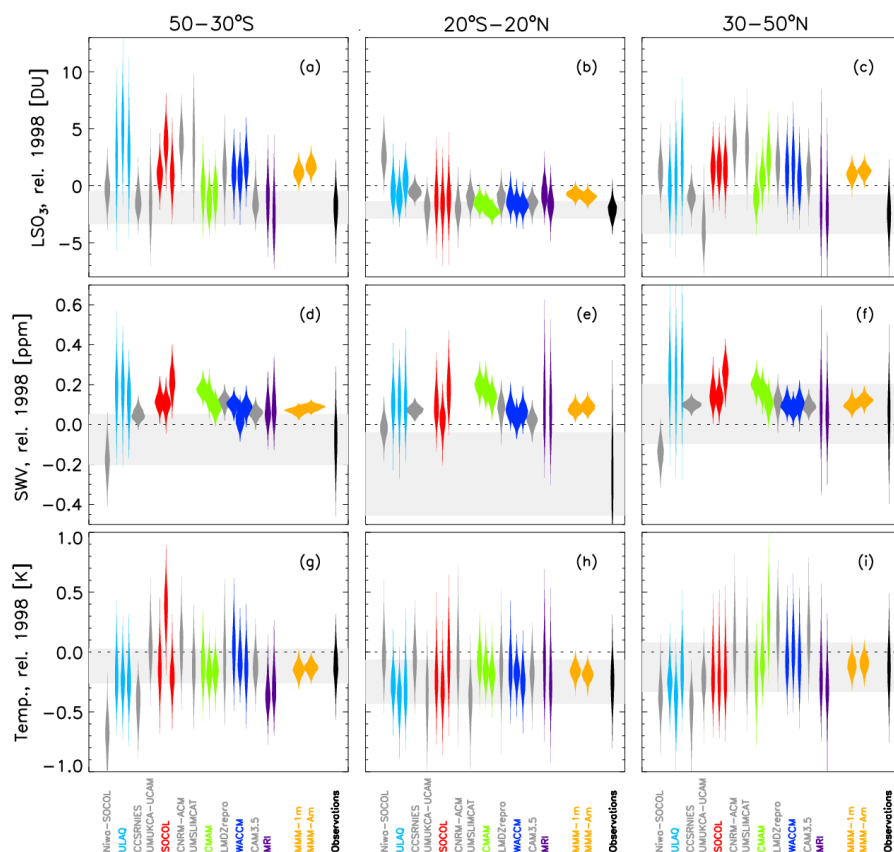
Figure 2: Lower stratospheric 1998–2016 ozone, water vapour, and temperature changes in models and observations. **(Left column)** 50–30°S, **(middle)** 20°S–20°N, and **(right)** 30–50°N; **(Upper row, a–c)** partial column ozone (147–32 hPa, 50–30°S/30–50°N); 100–32 hPa 20°N–20°S), **(middle, d–f)** stratospheric water vapour (SWV) at 83 hPa; **(lower, g–i)** temperature estimated from the MSU4 observing kernel. Violins represent double-sided probability distribution functions. Observations are black (right) with grey-bands representing the 68% highest density (most likely) interval; models are grey (single member ensembles) and colours are for models with more than one ensemble.

decrease than the MMM. At mid-latitudes (Figs. 2a, c), however, the MMM indicates a significant
265 increase, while observations show a decrease. It is this opposing behaviour at mid-latitudes, and the
smaller MMM decrease in the tropics, that leads to the opposing trends in the integrated quasi-global
lower stratospheric ozone (Fig. 1a, c). We therefore need to consider the equatorial and mid-latitude
changes separately.

3.2 Dynamics: evidence for increased tropical upwelling and mid-latitude mixing

270   The decrease in tropical ozone shown by most CCMs can be explained by an increase in tropical residual upwelling; upwelling is inversely correlated with tropical ozone over 1960–2100 in CCMVal-2 simulations (Fig. S11 of Eyring et al. (2010) and Fig. 9.6 of SPARC/WMO (2010)). It is well-established that later in the 21st Century a decline in tropical lower stratospheric ozone should emerge due to an acceleration of the large-scale Brewer-Dobson circulation (BDC) (Hardiman et al.,

275   2014; Butchart, 2014). This tropical lower stratospheric ozone decrease is actually already apparent in the spatially resolved changes presented in Fig. 3 in most CCMs. The magnitude of change is smaller in the MMM (Fig. 3b; see also WMO (2014) considering 2000–2013) compared to most of the individual CCMs (Fig. 3c–k), and observations (Fig. 3a) (WMO, 2014). The reason for a smaller tropical lower stratosphere ozone MMM decrease is because the magnitude and position of maxi-

280   mum decrease varies by CCM, and Niwa-SOCOL and ULAQ even show opposing, positive ozone changes (Fig. 3m–n). Overall, the implication is that at least part of the observed tropical lower stratospheric ozone decrease over 1998-2016 is likely to be driven by an acceleration of the BDC.

To determine whether a BDC acceleration is indeed driving the the lower stratospheric ozone decrease, we analyse 1998–2017 upwelling changes in two reanalysis products (JRA-55 (Ebita et al.,

285   2011) and ERA-Interim (Dee et al., 2011)), which represent observed historical changes in the circulation, at pressure levels just above the tropopause in Fig. 4b. We see an increase in residual upwelling at 96 hPa, which is highly likely (≥98% probability) in both reanalyses and approximately five times larger in magnitude than the CCMVal-2 models (not shown). At 80 and 67 hPa we see a likely (>90%) residual upwelling increase in JRA-55, while ERA-Interim shows decreasing confi-

290   dence with height. The 1998-2017 timeseries is short compared with the large interannual variability; using longer timeseries (1979–2017) to better constrain regressors does not change the conclusions. Therefore, our results provide evidence that enhanced upwelling, likely related to GHGs, i.e. climate change, has already been driving a tropical ozone decrease over 1998–2017 in both CCMs (Eyring et al., 2010; SPARC/WMO, 2010; Polvani et al., 2018, 2017) and observations (Ball et al., 2018, in

295   review, 2019).

At mid-latitudes (30-50°N/S), three CCMs display some decrease over the 1998-2016 period (Fig. 3). Notably, UMUKCA-UCAM and MRI display mid-latitude decreases (Fig. 2a,c) and spatial patterns (Fig. 3j,k) most reminiscent of the observations. Nevertheless, eight other CCMs suggest mid-latitude ozone increases consistent with enhanced downwelling in the shallow branch of

300   the BDC. These differences at mid-latitudes lead to the MMM and observations disagreeing in the quasi-global mean. To understand this discrepancy, we turn to other lower stratospheric variables.

It has been recently noted that the negative ozone trends in the lower stratosphere may be a result of enhanced isentropic mixing between the tropics and mid-latitudes, based on MERRA-2 reanalysis (Wargan et al., 2018), although in that study mixing was not explicitly calculated, whereas we

305   will do so here. Interestingly the UMUKCA-METO CCM, similar to UMUKCA-UCAM (differing
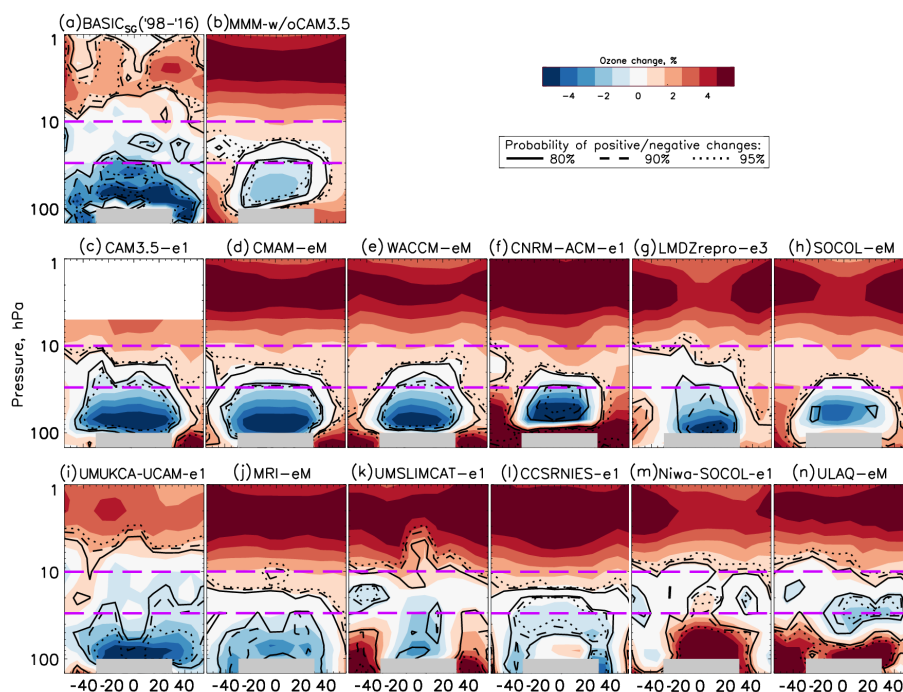
Figure 3: Latitude-pressure ozone changes from 1998–2016. **(a)** Observations, **(b)** CCMVal-2 MMM without CAM3.5, and **(c–n)** ensemble mean (eM) and single ensemble members (e1/e3) from each CCMVal-2 model. Colours represent positive (red) and negative (blue) changes (upper legend); contours represent probabilities of a positive or negative change (lower legend); grey shading represents the tropical troposphere, which is omitted. All changes are calculated considering only data from 1998–2016. All individual members of ensemble means are shown in Fig. S4; MMM results including CAM3.5 and a sensitivity test without five models are provided in Fig. S5.

primarily in how halogen washout and aerosol heating is treated (SPARC/WMO, 2010)), displays much larger mixing efficiency (Dietmüller et al., 2017) than any other CCM[1]. MRI also displays above average mixing efficiency relative to other CCMVal-2 models (Dietmüller et al., 2017). Both the large-scale BDC transport and mixing are expected to increase in the future (SPARC/WMO, 2010; Abalos et al., 2017). The implication, then, is that MRI and UMUKCA-UCAM display mid-latitude ozone decreases because of higher mixing efficiency in these models, and vice versa for the majority of CCMs.

---

[1]This includes models used in the chemistry climate model initiative phase 1 (CCMI-1 (Morgenstern et al., 2017)), updated since the chemistry climate model validation phase 2 (CCMVal-2 (SPARC/WMO, 2010)) models used here.
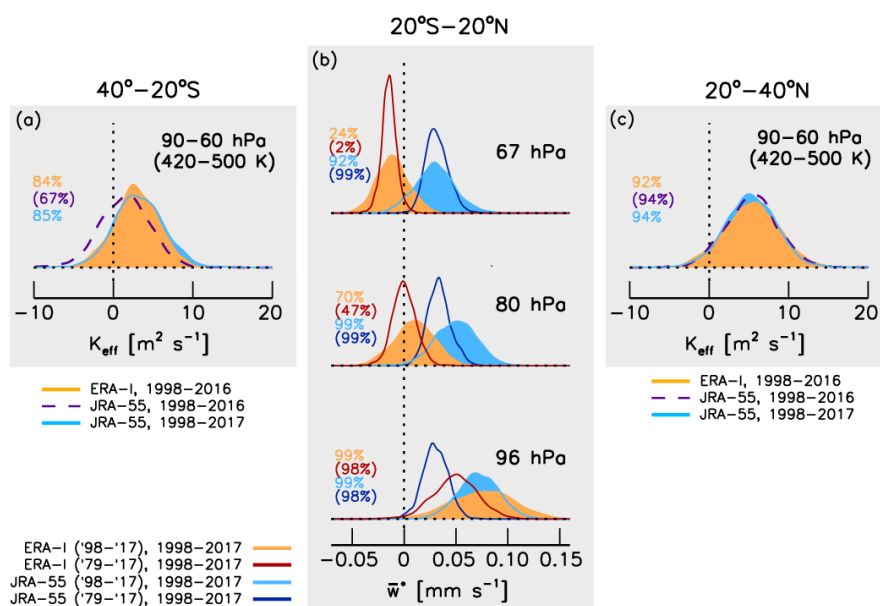
Figure 4: Effective latitudinal mixing and tropical upwelling changes since 1998. **(a)** southern hemisphere latitude-pressure averaged changes in latitudinal mixing, K_{eff} (40–20°S); **(c)** as for (a) but for northern latitudes (20–40°N). **(b)** tropical (20°N–20°S) upwelling changes ($\overline{w}^*$) at three pressure levels: **(top)** 67 hPa, **(middle)** 80 hPa, and **(bottom)** 96 hPa. Estimates are made from reanalysis for periods in the legends. In (b), solid probability distribution functions (PDFs) are for changes estimated using data covering 1998–2017, while line-PDFs are using 1979–2017; for (a) and (c) ERA-Interim has a solid PDF for 1998–2016, while JRA-55 has a solid (line) PDF for 1998–2017 (1998–2016). Percentages are the probability of positive changes in all PDFs; brackets surround percentages for the line PDFs. Timeseries for (b) are provided in Fig. S6; Fig. S7 for (a,c).

In addition to previous work considering MERRA-2 reanalysis (Wargan et al., 2018), we provide further supporting observational evidence that mixing has increased since 1998 using JRA-55 and
315   ERA-Interim reanalyses. Figs. 4a and 4c indicate that mixing across the sub-tropics between the equator and the SH and NH, respectively, increased over 1998–2016 (and 1998-2017) in both ERA-Interim and JRA-55 reanalyses (estimated from effective diffusivity (Haynes and Shuckburgh, 2000; Abalos et al., 2016) in Fig. S7). The increase in mixing is larger and more probable in the NH (>92%) than the SH (>66%), which is in agreement with the NH displaying larger mid-latitude
320   decreases than the SH (Ball et al., 2018; Chipperfield et al., 2018; Wargan et al., 2018; Ball et al., in review, 2019). Thus, there is now consistent observational evidence in support of enhanced mixing to mid-latitudes in the recent past.

13

3.3 Temperature: imprints of decreasing ozone

The aforementioned changes in ozone and transport, if correct, should be found in other stratospheric
variables: ozone is not an isolated quantity, and the 1998–2016 reduction in lower stratospheric
ozone should lead to reduced radiative heating and a decrease in observed temperature (London,
1980; Brasseur and Solomon, 2005). Quasi-global lower stratospheric temperature from observations (see Methods) is shown in Fig. 1a; the temperature evolution mimics the pre-1998 ozone decreases, flattening through the 2000s, and then continuing to decrease after 2009; the behaviour of the
acceleration curve (Fig. 1c) also follows the variations in ozone post-2002, as expected physically.
A recent analysis of updated temperature trends (Maycock et al., 2018) concluded that the negative
1998–2016 temperature trend was smaller compared to 1979–1997, as a result of reduced loss of
ozone, caused by a phase-out of ODS emissions; the qualitatively consistent ozone and temperature
trends (Fig. 1c) supports this conclusion. By 2016, observed quasi-global temperature (60°S–60°N)
is approximately 0.20 K lower than in 1998 (Fig. 1a); the same is true for the MMM (0.15 K; Fig. 1b),
and across latitude bands (SH, tropical, and NH; Fig. 2g–i) for individual CCMs.

However, while temperature trends are consistent with ozone in the tropics, there are inconsistencies in the mid-latitudes, where MMM and observed 1998–2016 temperature changes agree with
observations, but ozone trends do not. To estimate the ozone contribution to the temperature decreases, we applied the FDH approximation scheme (section 2.5) to the spatially-resolved observed
(Fig. 5a) and MMM (Fig. 5b) 1998–2016 ozone changes within a CCM (Fig. 5d,h; see Methods), and
then applied the MSU temperature observing kernel to yield the ozone contribution to the temperature decrease (Fig. 5e, j); the MSU4 kernel as presented in (Randel et al., 2009) is plotted in Fig. 5
between panels f and g. We note that FDH provides a first-order estimate of the ozone contribution
to temperature changes, as it neglects non-radiative processes such as dynamical adjustments. We
find that the FDH estimated ozone contribution to the observed temperature change agrees with the
observed latitudinal temperature changes (Fig. 5e) and that the 60°S–60°N integrated FDH estimate
yields an ozone contribution to the temperature change of -0.24 K. The coherent changes in ozone
and temperature in observations (Fig. 1a), along with the FDH calculations confirm that ozone is
the major contributor to the observed temperature decreases (Fig. 5e). The story is different when
applying the FDH approximation to the MMM ozone changes: as expected, tropical ozone decreases
should lead to cooling (Fig. 5j), but the mid-latitude ozone increase is inconsistent with the temperature decrease in the MMM, and the 60°S–60°N quasi-global FDH temperature change induced by
ozone is only ~+0.01 K. Therefore, for this to be physically consistent with the MMM 1998–2016
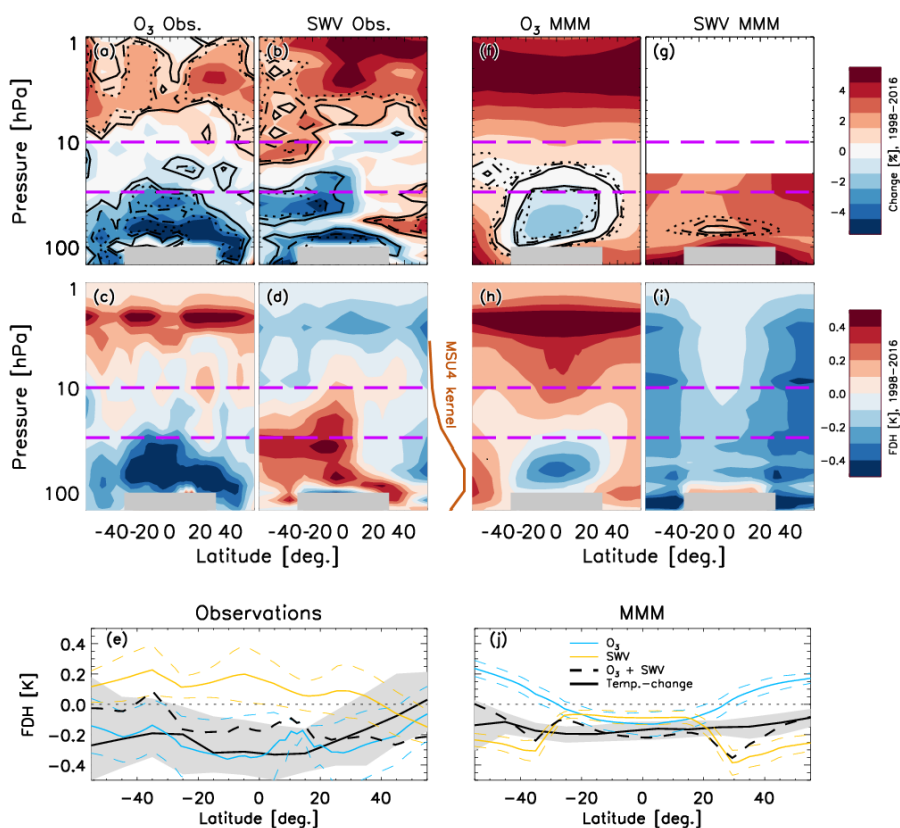temperature decreases, something else must be driving the lower stratospheric cooling in CCMs.

Figure 5: Fixed dynamical heating estimate of ozone and SWV contribution to lower stratosphere temperature changes. **(a–e)** Observed and **(f–j)** MMM estimates for **(a,f)** ozone and **(b,g)** SWV changes (right legend), the corresponding spatially resolved FDH-estimated contributions to temperature changes from **(c,h)** ozone and **(d,i)** SWV temperature; **(e,j)** after applying the MSU4 observing kernel, the estimated latitudinal contribution to MSU4 temperature changes with 68% credible intervals; the MSU4 kernel (Randel et al., 2009) is plotted between panels d and h.

3.4 Stratospheric water vapour: reconciling observed and modelled temperature trends

In addition to ozone, stratospheric temperatures are affected by radiative effects from, and chemical changes in, CO_2, N_2O, and CH_4 (Revell et al., 2012; Portmann et al., 2012; Nowack et al., 2015) and stratospheric water vapor (SWV) (Forster and Shine, 1999; Dessler et al., 2013). While cooling
360   from CO_2 is important in the upper stratosphere, near the tropopause it has little relative contribution (Shine et al., 2003; Brasseur and Solomon, 2005; Maycock et al., 2011). SWV is the next most important contributor to lower stratospheric temperature changes and has the opposite effect on temperature to ozone in the lower stratosphere, i.e. cooling if SWV increases (Shine et al., 2003; Brasseur and Solomon, 2005; Maycock et al., 2011). For the FDH-estimated ozone contribution to
365   temperature changes to be consistent across latitudes (Fig. 5), SWV in the MMM would need to increase after 1998 (Gettelman et al., 2010), while observed SWV (Davis et al., 2016) needs to change little or decrease slightly by 2016. This is exactly what we find: MMM SWV at 83 hPa (close to the peak of the observing kernel of the MSU4 temperature observations; Fig. 5) increases almost linearly over 1985–2016 (Fig. 1b), while SWV in observations shows a continuous decrease from 1994,
370   flattening slightly after 2000 (Fig. 1a); the picture is more nuanced across latitude bands (Fig. 2d–f). Observed quasi-global SWV decreases are dominated by the tropics (Fig. 2e), which is also where the discrepancy between SWV trends in the MMM and observations is largest. The observed changes in SWV lead to hemispheric differences in the FDH estimated contribution to temperature (Fig. 5e), with overestimation at Northern latitudes, and underestimation in the tropics and Southern latitudes
375   (though remain within the 68% credible intervals). The FDH-estimated SWV contribution to the MMM temperature changes lead to improved agreement with the MMM temperature change and with observations (Fig. 5j); the quasi-global FDH estimate for SWV in the observations and MMM is +0.10 and -0.16 K, respectively. The combined quasi-global ozone and SWV contributions to the observed and MMM temperature changes are in agreement within uncertainties, i.e. -0.14 and -0.15
380   K respectively (Figs. 5e, j), and with the directly observed quasi-global cooling (Fig. 1a). Therefore, while the contribution of SWV and ozone to temperature changes over 1998-2016 in the MMM do not agree with observations at mid-latitutdes, their opposing tendencies offset each other and lead to a coincidental agreement in temperature.

SWV changes are not required to explain the observed temperature changes (using FDH, within
385   the uncertainties), but are required to explain the MMM-observation agreement in temperature in spite of opposing ozone trends. The enhanced upwelling should lead to cooling, which is not included in the FDH estimate, and might be a missing component in the difference between the combined FDH SWV-ozone contribution to the temperature change (Fig. 5e). The difference in FDH-estimated observation-model temperature changes, as well as the larger uncertainties in the
390   FDH-estimate from observations, could be explained by natural variability in the observations that is suppressed in the MMM from averaging natural variability over multiple models. In summary, the

temperature changes in the MMM and observations agree fortuitously over the 1998-2016 period, since the changes in trace gases driving those temperature changes disagree.

3.5 Discussion

395 Bringing together all of the results presented here – ozone, temperature, SWV, upwelling, and mixing – we can hypothesize the likely mechanism driving the long-term changes in the lower stratosphere. Tropical upwelling appears to be increasing (Fig. 4b), and modelling studies indicate this to result from increased GHGs (Eyring et al., 2010; Polvani et al., 2018) that drive climate change. This directly leads to a decrease in tropical lower stratospheric ozone (Fig. 2b). Further evidence suggests

400 that mixing of air from the ozone-poor tropical lower stratosphere to mid-latitudes has enhanced (Fig. 4a,c), and we conclude that this is a probable cause of the observed ozone decreases at mid-latitudes (Fig. 4a,c). The consequence is that the continuing ozone decrease is driving the majority of the ongoing temperature decrease in the lower stratosphere at tropical and mid-latitudes (Figs. 2g–i and 5e) (Maycock et al., 2018), as the FDH calculations confirm. Most CCMs reproduce the tropical

405 upwelling and associated ozone decrease (SPARC/WMO, 2010), but CCMs with higher mixing efficiency (Dietmüller et al., 2017) produce ozone trends more similar to the observations at mid-latitudes (Figs. 2a-c and 3). The role of enhanced mixing in driving ozone trends at mid-latitudes is supported by the observational results estimated from reanalyses (Fig. 4a,c). Further, the temperature decreases in CCMs agree with observations (Fig. 2g–i) because SWV is increasing in the CCMs

410 (Figs. 1 and 2) and thus cooling the mid-latitude lower stratosphere (Fig. 5j); observations show no confident change in SWV at mid-latitudes (Fig. 2d,f), though we do not have an explanation as to why modelled SWV changes do not agree with observations.

However, many caveats and open questions remain. The mechanism proposed here – with SWV and ozone driving the majority of temperature changes – does not fully explain the different changes

415 in temperature between each CCM (Fig. 2); this will require a deeper, case by case examination of how each model is operating. The CCMs considered here are a part of the CCMVal-2 model intercomparison that preceeds the more recent CCMI-1, but nevertheless other studies have shown that results between CCMVal-2 and CCMI-1 are consistent in their multi-decadal changes in SWV (Smalley et al., 2017), ozone (Dhomse et al., 2018), temperature (Maycock et al., 2018), and with

420 upwelling and mixing (Dietmüller et al., 2017), and are therefore still representative of the state-of-the-art. The CCM simulations analyzed in this study also mainly consider long-term changes in ODSs and GHGs, but do not prescribe the observed sea surface temperatures, which means natural variability in temperature is likely different to that of the observed world. As such, the effect of large natural variability affecting the temperature trend estimates is not taken into account in this study

425 (Ball et al., in review, 2019); whether natural variability or the GHG forcing signal is underestimated in the CCMs, and is the cause of the difference with observations, remains an open question. We note that this has been discussed in several recent studies (Ball et al., 2018; Chipperfield et al.,

2018; Wargan et al., 2018; Stone et al., 2018), but an update in ozone trends shows that the observed negative lower stratospheric ozone trends persist despite large interannual variability (Ball et al., in review, 2019). Further, one might expect decreasing temperatures near the tropical tropopause entry point to freeze-out more water vapour from air entering the lower stratosphere. However, this is not what CCMs show, and the temperature changes at the entry point is hard to predict due to stratospheric cooling, tropospheric warming, and a rise of the tropopause (Gettelman et al., 2009; WMO, 2018), as well as other processes such as convective over-shooting and isentropic mixing with mid-latitudes complicating the picture further. The large altitude range of the MSU-4 kernels applied to the CCMs that includes the upper troposphere may hide a rising or warming tropopause region (SPARC/WMO, 2010), inhibiting attribution to the cause. Numerical diffusion in CCMs might also allow water vapour to incorrectly enter the lower stratosphere in models and should also be considered for further evaluation. Finally, multi-decadal (natural) variability is an alternative hypothesis to the signals presented here being climate-change driven, although a specific internal driver to attribute the signal is not currently available, so GHG increases remain, in our view, the more likely hypothesis at this stage.

4 Conclusions

In summary, we have presented results that show the behaviour of decreasing ozone in the lower stratosphere appears to be imprinted on temperature changes and might be explained by enhanced upwelling and increased horizontal mixing; at least part of the tropical changes can be attributed through models to an acceleration of the BDC due to rising GHGs (SPARC/WMO, 2010; Polvani et al., 2018). Tropospheric temperature increases due to increased GHG emissions modify the thermal wind balance and strengthen the sub-tropical jets in the lower stratosphere, which subsequently affect wave dissipation (Garcia and Randel, 2008; Shepherd and McLandress, 2011) that directly influences the strength of upwelling and mixing (Wargan et al., 2018) in the lower stratosphere. If ozone decreases in the tropical lower stratosphere and then mixing and transport to mid-latitudes is enhancing, as we indeed find, a decrease in ozone both in the tropics and mid-latitudes is the expected, and observed, outcome (Ball et al., 2018). Our results suggest that the quasi-global lower stratospheric ozone decline can be explained by climate-change related changes in transport and mixing in the lower stratosphere.

However, confidence in future projections using CCMs relies on agreement with observations over the historical record; indeed, the two CCMs displaying mid-latitude decreases (MRI and UMUKCA-UCAM) do project a mid-latitude recovery by the middle of this century (Fig. S8). However, since we do not yet know why CCMs in general do not reproduce the observed ozone decreases in the mid-latitudes, or indeed why these two do, open questions remain about the future of lower stratospheric ozone and the ozone layer under a changing climate.

Atmospheric
Chemistry
and Physics
Discussions

Author contributions. G.C. prepared the model data, W.T.B prepared the observational data, and W.T.B. and
J.A. performed the DLM analysis; W.T.B and J.A. did the statistical analysis. G.C. performed the FDH calcu-

465 lations. M.A. prepared ERA-Interim and JRA-55 reanalyses, and calculated mixing and upwelling variables.
W.T.B. prepared figures and wrote the manuscript. All authors contributed to the manuscript.

References

Abalos, M., Legras, B., and Shuckburgh, E.: Interannual variability in effective diffusivity in the upper tropo-sphere/lower stratosphere from reanalysis data, Quarterly Journal of the Royal Meteorological Society, 142, 1847–1861, doi:10.1002/qj.2779, 2016.

475 Abalos, M., Randel, W. J., Kinnison, D. E., and Garcia, R. R.: Using the Artificial Tracer e90 to Examine Present and Future UTLS Tracer Transport in WACCM, Journal of Atmospheric Sciences, 74, 3383–3403, doi:10.1175/JAS-D-17-0135.1, 2017.

Alsing, J.: dlmmc: Dynamical linear model regression for atmospheric time-series analysis, Journal of Open Source Software, 4(37), 1157, doi:10.21105/joss.01157, 2019.

480 Alsing, J. and Ball, W. T.: BASIC Composite Ozone Time-Series Data version 2, doi:10.17632/2mgx2xzzpk.2, 2017.

Ball, W. T., Alsing, J., Mortlock, D. J., Rozanov, E. V., Tummon, F., and Haigh, J. D.: Reconciling differences in stratospheric ozone composites, Atmospheric Chemistry & Physics, 17, 12 269–12 302, doi:10.5194/acp-17-12269-2017, 2017.

485 Ball, W. T., Alsing, J., Mortlock, D. J., Staehelin, J., Haigh, J. D., Peter, T., Tummon, F., Stuebi, R., Stenke, A., Anderson, J., Bourassa, A., Davis, S. M., Degenstein, D., Frith, S., Froidevaux, L., Roth, C., Sofieva, V., Wang, R., Wild, J., Yu, P., Ziemke, J. R., and Rozanov, E. V.: Evidence for a continuous decline in lower stratospheric ozone offsetting ozone layer recovery, Atmospheric Chemistry & Physics, 18, 1379–1394, doi:10.5194/acp-18-1379-2018, 2018.

490 Ball, W. T., Alsing, J., Staehelin, J., Davis, S. M., Froidevaux, L., and Peter, T.: Stratospheric ozone trends for 1985–2018: sensitivity to recent large variability, Atmos. Chem. Phys. Disc., doi:10.5194/acp-2019-243, in review, 2019.

Bourassa, A. E., Roth, C. Z., Zawada, D. J., Rieger, L. A., McLinden, C. A., and Degenstein, D. A.: Drift corrected Odin-OSIRIS ozone product: algorithm and updated stratospheric ozone trends, Atmos. Meas.
495 Tech. Discuss., doi:10.5194/amt-2017-229, 2017.

Brasseur, G. P. and Solomon, S.: Aeronomy of the Middle Atmosphere: Chemistry and Physics of the Strato-sphere and Mesosphere, Dordrecht: Springer Netherlands, Editor: Mysak, L. A., 2005.

Butchart, N.: The Brewer-Dobson circulation, Reviews of Geophysics, 52, 157–184, doi:10.1002/2013RG000448, 2014.

500 Chehade, W., Weber, M., and Burrows, J. P.: Total ozone trends and variability during 1979-2012 from merged data sets of various satellites, Atmospheric Chemistry & Physics, 14, 7059–7074, doi:10.5194/acp-14-7059-2014, 2014.

Chipperfield, M. P., Dhomse, S. S., Feng, W., McKenzie, R. L., Velders, G. J. M., and Pyle, J. A.: Quantifying the ozone and ultraviolet benefits already achieved by the Montreal Protocol, Nature Communications, 6,
505 7233, doi:10.1038/ncomms8233, 2015.

Chipperfield, M. P., Bekki, S., Dhomse, S., Harris, N. R. P., Hassler, B., Hossaini, R., Steinbrecht, W., Thiéble-mont, R., and Weber, M.: Detecting recovery of the stratospheric ozone layer, Nature, 549, 211–218, doi:10.1038/nature23681, 2017.

Chipperfield, M. P., Dhomse, S., Hossaini, R., Feng, W., Santee, M. L., Weber, M., Burrows, J. P., Wild, J. D.,
510   Loyola, D., and Coldewey-Egbers, M.: On the Cause of Recent Variations in Lower Stratospheric Ozone,
       Geophys. Res. Lett., 45, 5718–5726, doi:10.1029/2018GL078071, 2018.

Conley, A., Lamarque, J.-F., Vitt, F., Collins, W., and Kiehl, J.: PORT, a CESM tool for the diagnosis of radiative
       forcing, Geoscientific Model Development, 6, 469–476, 2013.

Davis, S. M., Rosenlof, K. H., Hassler, B., Hurst, D. F., Read, W. G., Vömel, H., Selkirk, H., Fujiwara, M., and
515   Damadeo, R.: The Stratospheric Water and Ozone Satellite Homogenized (SWOOSH) database: a long-term
       database for climate studies, Earth System Science Data, 8, 461–490, doi:10.5194/essd-8-461-2016, 2016.

Dee, D. P., Uppala, S. M., Simmons, A. J., Berrisford, P., Poli, P., Kobayashi, S., Andrae, U., Balmaseda,
       M. A., Balsamo, G., Bauer, P., Bechtold, P., Beljaars, A. C. M., van de Berg, L., Bidlot, J., Bormann, N.,
       Delsol, C., Dragani, R., Fuentes, M., Geer, A. J., Haimberger, L., Healy, S. B., Hersbach, H., Hólm, E. V.,
520   Isaksen, L., Kållberg, P., Köhler, M., Matricardi, M., McNally, A. P., Monge-Sanz, B. M., Morcrette, J.-
       J., Park, B.-K., Peubey, C., de Rosnay, P., Tavolato, C., Thépaut, J.-N., and Vitart, F.: The ERA-Interim
       reanalysis: configuration and performance of the data assimilation system, Quarterly Journal of the Royal
       Meteorological Society, 137, 553–597, doi:10.1002/qj.828, 2011.

Dessler, A. E., Schoeberl, M. R., Wang, T., Davis, S. M., and Rosenlof, K. H.: Stratospheric water vapor
525   feedback, PNAS, 110, 18 087–18 091, doi:doi.org/10.1073/pnas.1310344110, 2013.

Dhomse, S. S., Kinnison, D., Chipperfield, M. P., Salawitch, R. J., Cionni, I., Hegglin, M. I., Abraham, N. L.,
       Akiyoshi, H., Archibald, A. T., Bednarz, E. M., Bekki, S., Braesicke, P., Butchart, N., Dameris, M., Deushi,
       M., Frith, S., Hardiman, S. C., Hassler, B., Horowitz, L. W., Hu, R.-M., Jöckel, P., Josse, B., Kirner, O.,
       Kremser, S., Langematz, U., Lewis, J., Marchand, M., Lin, M., Mancini, E., Marécal, V., Michou, M., Mor-
530   genstern, O., O'Connor, F. M., Oman, L., Pitari, G., Plummer, D. A., Pyle, J. A., Revell, L. E., Rozanov,
       E., Schofield, R., Stenke, A., Stone, K., Sudo, K., Tilmes, S., Visioni, D., Yamashita, Y., and Zeng, G.: Es-
       timates of ozone return dates from Chemistry-Climate Model Initiative simulations, Atmospheric Chemistry
       & Physics, 18, 8409–8438, doi:10.5194/acp-18-8409-2018, 2018.

Dietmüller, S., Garny, H., Plöger, F., Jöckel, P., and Cai, D.: Effects of mixing on resolved and unresolved
535   scales on stratospheric age of air, Atmospheric Chemistry & Physics, 17, 7703–7719, doi:10.5194/acp-17-
       7703-2017, 2017.

Douglass, A. R., Stolarski, R. S., Strahan, S. E., and Oman, L. D.: Understanding differences in upper strato-
       spheric ozone response to changes in chlorine and temperature as computed using CCMVal-2 models, Journal
       of Geophysical Research (Atmospheres), 117, D16306, doi:10.1029/2012JD017483, 2012.

540   Douglass, A. R., Strahan, S. E., Oman, L. D., and Stolarski, R. S.: Understanding differences in chemistry
       climate model projections of stratospheric ozone, Journal of Geophysical Research (Atmospheres), 119,
       4922–4939, doi:10.1002/2013JD021159, 2014.

Dudok de Wit, T., Bruinsma, S., and Shibasaki, K.: Synoptic radio observations as proxies for upper atmosphere
       modelling, Journal of Space Weather and Space Climate, 4, A06, doi:10.1051/swsc/2014003, 2014.

545   Ebita, A., Kobayashi, S., Ota, Y., Moriya, M., Kumabe, R. Onogi, K., Harada, Y., Yasui, S., Miyaoka, K.,
       Takahashi, K., Kamahori, H., Kobayashi, C., Endo, H., Soma, M., Oikawa, Y., and Ishimizu, T.: The Japanese
       55-year reanalysis (JRA-55): An Interim Report, Sola, 7, 2011.

Egorova, T., Rozanov, E., Gröbner, J., Hauser, M., and Schmutz, W.: Montreal Protocol Benefits simulated with CCM SOCOL, Atmospheric Chemistry & Physics, 13, 3811–3823, doi:10.5194/acp-13-3811-2013, 2013.

550   Eyring, V., Cionni, I., Bodeker, G. E., Charlton-Perez, A. J., Kinnison, D. E., Scinocca, J. F., Waugh, D. W., Akiyoshi, H., Bekki, S., Chipperfield, M. P., Dameris, M., Dhomse, S., Frith, S. M., Garny, H., Gettelman, A., Kubin, A., Langematz, U., Mancini, E., Marchand, M., Nakamura, T., Oman, L. D., Pawson, S., Pitari, G., Plummer, D. A., Rozanov, E., Shepherd, T. G., Shibata, K., Tian, W., Braesicke, P., Hardiman, S. C., Lamarque, J. F., Morgenstern, O., Pyle, J. A., Smale, D., and Yamashita, Y.: Multi-model assessment
555   of stratospheric ozone return dates and ozone recovery in CCMVal-2 models, Atmospheric Chemistry & Physics, 10, 9451–9472, doi:10.5194/acp-10-9451-2010, 2010.

Fels, S., Mahlman, J., Schwarzkopf, M., and Sinclair, R.: Stratospheric sensitivity to perturbations in ozone and carbon dioxide: Radiative and dynamical response, Journal of the Atmospheric Sciences, 37, 2265–2297, 1980.

560   Forster, P. J. and Shine, K. P.: Stratospheric water vapour changes as a possible contributor to observed stratospheric cooling, Geophysical research letters, 26, 3309–3312, 1999.

Forster, P. M. and Shine, K. P.: Radiative forcing and temperature trends from stratospheric ozone changes, Journal of Geophysical Research: Atmospheres, 102, 10 841–10 855, 1997.

Frith, S. M., Kramarova, N. A., Stolarski, R. S., McPeters, R. D., Bhartia, P. K., and Labow, G. J.: Recent
565   changes in total column ozone based on the SBUV Version 8.6 Merged Ozone Data Set, Journal of Geophysical Research (Atmospheres), 119, 9735–9751, doi:10.1002/2014JD021889, 2014.

Froidevaux, L., Anderson, J., Wang, H.-J., Fuller, R. A., Schwartz, M. J., Santee, M. L., Livesey, N. J., Pumphrey, H. C., Bernath, P. F., Russell, III, J. M., and McCormick, M. P.: Global OZone Chemistry And Related trace gas Data records for the Stratosphere (GOZCARDS): methodology and sample results with
570   a focus on HCl, H_2O, and O_3, Atmospheric Chemistry & Physics, 15, 10 471–10 507, doi:10.5194/acp-15-10471-2015, 2015.

Froidevaux, L., Kinnison, D. E., Wang, R., Anderson, J., and Fuller, R. A.: Evaluation of CESM1 (WACCM) free-running and specified-dynamics atmospheric composition simulations using global multispecies satellite data records, Atmos. Chem. Phys., 19, 4783–4821, doi:10.5194/acp-19-4783-2019, 2019.

575   Garcia, R. R. and Randel, W. J.: Acceleration of the Brewer-Dobson Circulation due to Increases in Greenhouse Gases, Journal of Atmospheric Sciences, 65, 2731–2739, doi:10.1175/2008JAS2712.1, 2008.

Gaudel, A., Cooper, O. R., and etc, E.: Tropospheric Ozone Assessment Report: Present-day distribution and trends of tropospheric ozone relevant to climate and global atmospheric chemistry model evaluation, Elem Sci Anth, 6, 10, doi:10.1525/elementa.291, 2018.

580   Gettelman, A., Birner, T., Eyring, V., Akiyoshi, H., Bekki, S., Brühl, C., Dameris, M., Kinnison, D. E., Lefevre, F., Lott, F., Mancini, E., Pitari, G., Plummer, D. A., Rozanov, E., Shibata, K., Stenke, A., Struthers, H., and Tian, W.: The Tropical Tropopause Layer 1960â€"2100, Atmospheric Chemistry and Physics, 9, 1621–1637, doi:10.5194/acp-9-1621-2009, https://www.atmos-chem-phys.net/9/1621/2009/, 2009.

Gettelman, A., Hegglin, M. I., Son, S.-W., Kim, J., Fujiwara, M., Birner, T., Kremser, S., Rex, M., AñEl,
585   J. A., Akiyoshi, H., Austin, J., Bekki, S., Braesike, P., Brühl, C., Butchart, N., Chipperfield, M., Dameris, M., Dhomse, S., Garny, H., Hardiman, S. C., JöCkel, P., Kinnison, D. E., Lamarque, J. F., Mancini, E., Marchand, M., Michou, M., Morgenstern, O., Pawson, S., Pitari, G., Plummer, D., Pyle, J. A., Rozanov, E.,

Scinocca, J., Shepherd, T. G., Shibata, K., Smale, D., TeyssèDre, H., and Tian, W.: Multimodel assessment of the upper troposphere and lower stratosphere: Tropics and global trends, Journal of Geophysical Research
590   (Atmospheres), 115, D00M08, doi:10.1029/2009JD013638, 2010.

Hardiman, S. C., Butchart, N., and Calvo, N.: The morphology of the Brewer-Dobson circulation and its response to climate change in CMIP5 simulations, Quarterly Journal of the Royal Meteorological Society, 140, 1958–1965, doi:10.1002/qj.2258, 2014.

Harris, N. R. P., Hassler, B., Tummon, F., Bodeker, G. E., Hubert, D., Petropavlovskikh, I., Steinbrecht, W.,
595   Anderson, J., Bhartia, P. K., Boone, C. D., Bourassa, A., Davis, S. M., Degenstein, D., Delcloo, A., Frith, S. M., Froidevaux, L., Godin-Beekmann, S., Jones, N., Kurylo, M. J., Kyrölä, E., Laine, M., Leblanc, S. T., Lambert, J.-C., Liley, B., Mahieu, E., Maycock, A., de Mazière, M., Parrish, A., Querel, R., Rosenlof, K. H., Roth, C., Sioris, C., Staehelin, J., Stolarski, R. S., Stübi, R., Tamminen, J., Vigouroux, C., Walker, K. A., Wang, H. J., Wild, J., and Zawodny, J. M.: Past changes in the vertical distribution of ozone - Part 3: Analysis
600   and interpretation of trends, Atmospheric Chemistry & Physics, 15, 9965–9982, doi:10.5194/acp-15-9965-2015, 2015.

Haynes, P. and Shuckburgh, E.: Effective diffusivity as a diagnostic of atmospheric transport: 2. Troposphere and lower stratosphere, J. Geophys. Res., 105, 22,795–22,810, doi:10.1029/2000JD900092, 2000.

Kobayashi, S., Ota, Y., Harada, Y., Ebita, A., Moriya, M., Onoda, H., Onogi, K., Kamahori, H., Kobayashi,
605   C., Endo, H., Miyaoka, K., and Takahashi, K.: The JRA-55 Reanalysis: General Specifications and Basic Characteristics, Journal of the Meteorological Society of Japan. Ser. II, 93, 5–48, doi:10.2151/jmsj.2015-001, 2015.

Laine, M., Latva-Pukkila, N., and Kyrölä, E.: Analysing time-varying trends in stratospheric ozone time series using the state space approach, Atmospheric Chemistry & Physics, 14, 9707–9725, doi:10.5194/acp-14-
610   9707-2014, 2014.

London, J.: Radiative Energy Sources and Sinks in the Stratosphere and Mesosphere, in: Atmospheric Ozone and its Variation and Human Influences, edited by Nicolet, M. and Aikin, A. C., p. 703, 1980.

Maycock, A. C., Shine, K. P., and Joshi, M. M.: The temperature response to stratospheric water vapour changes, Quarterly Journal of the Royal Meteorological Society, 137, 1070–1082, doi:10.1002/qj.822, 2011.

615   Maycock, A. C., Randel, W. J., Steiner, A. K., Karpechko, A. Y., Christy, J., Saunders, R., Thompson, D. W. J., Zou, C.-Z., Chrysanthou, A., Luke Abraham, N., Akiyoshi, H., Archibald, A. T., Butchart, N., Chipperfield, M., Dameris, M., Deushi, M., Dhomse, S., Di Genova, G., Jöckel, P., Kinnison, D. E., Kirner, O., Ladstädter, F., Michou, M., Morgenstern, O., O'Connor, F., Oman, L., Pitari, G., Plummer, D. A., Revell, L. E., Rozanov, E., Stenke, A., Visioni, D., Yamashita, Y., and Zeng, G.: Revisiting the Mystery of Recent Stratospheric
620   Temperature Trends, Geophys. Res. Lett., 45, 9919–9933, doi:10.1029/2018GL078035, 2018.

Morgenstern, O., Hegglin, M. I., Rozanov, E., O'Connor, F. M., Abraham, N. L., Akiyoshi, H., Archibald, A. T., Bekki, S., Butchart, N., Chipperfield, M. P., Deushi, M., Dhomse, S. S., Garcia, R. R., Hardiman, S. C., Horowitz, L. W., Jöckel, P., Josse, B., Kinnison, D., Lin, M., Mancini, E., Manyin, M. E., Marchand, M., Marécal, V., Michou, M., Oman, L. D., Pitari, G., Plummer, D. A., Revell, L. E., Saint-Martin, D.,
625   Schofield, R., Stenke, A., Stone, K., Sudo, K., Tanaka, T. Y., Tilmes, S., Yamashita, Y., Yoshida, K., and Zeng, G.: Review of the global models used within phase 1 of the Chemistry-Climate Model Initiative (CCMI), Geoscientific Model Development, 10, 639–671, doi:10.5194/gmd-10-639-2017, 2017.

Atmospheric
Chemistry
and Physics
Discussions

Newman, P. A., Daniel, J. S., Waugh, D. W., and Nash, E. R.: A new formulation of equivalent effective strato-
spheric chlorine (EESC), Atmospheric Chemistry & Physics, 7, 4537–4552, 2007.

630 Nowack, P. J., Luke Abraham, N., Maycock, A. C., Braesicke, P., Gregory, J. M., Joshi, M. M., Osprey, A., and
Pyle, J. A.: A large ozone-circulation feedback and its implications for global warming assessments, Nature
Climate Change, 5, 41–45, doi:10.1038/nclimate2451, 2015.

Pazmino, A., Godin-Beekmann, S., Hauchecorne, A., Claud, C., Khaykin, S., Goutail, F., Wolfram, E., Salvador,
J., and Quel, E.: Symptoms of total ozone recovery inside the Antarctic vortex during Austral spring, Atmos.

635 Chem. Phys. Discuss., doi:10.5194/acp-2017-1157, 2017.

Penckwitt, A. A., E., B. G., Revell, L. E., Richter, L., Kyrölä, E., and Young, P.: Construction and analysis of
a new merged SAGE II-GOMOS ozone profile data set for 1984-2012, Earth Syst. Sci. Data, in preparation,
2015.

Petropavlovskikh, I., Godin-Beekmann, S., Hubert, D., Damadeo, R., Hassler, B., and Sofieva,

640 V.: SPARC/IO3C/GAW report on Long-term Ozone Trends and Uncertainties in the Strato-
sphere, SPARC/IO3C/GAW, SPARC Report No. 9, WCRP-17/2018, GAW Report No. 241,
doi:10.17874/f899e57a20b, 2019.

Polvani, L. M., Wang, L., Aquila, V., and Waugh, D. W.: The Impact of Ozone-Depleting Substances on Tropical
Upwelling, as Revealed by the Absence of Lower-Stratospheric Cooling since the Late 1990s, Journal of

645 Climate, 30, 2523–2534, doi:10.1175/JCLI-D-16-0532.1, 2017.

Polvani, L. M., Abalos, M., Garcia, R., Kinnison, D., and Randel, W. J.: Significant Weakening of Brewer-
Dobson Circulation Trends Over the 21st Century as a Consequence of the Montreal Protocol, Geophys.
Res. Lett., 45, 401–409, doi:10.1002/2017GL075345, 2018.

Portmann, R. W., Daniel, J. S., and Ravishankara, A. R.: Stratospheric ozone depletion due to nitrous oxide:

650 influences of other gases, Philos Trans R Soc Lond B Biol Sci., 367, 1256–1264, 2012.

Randel, W. J., Shine, K. P., Austin, J., Barnett, J., Claud, C., Gillett, N. P., Keckhut, P., Langematz, U., Lin,
R., Long, C., Mears, C., Miller, A., Nash, J., Seidel, D. J., Thompson, D. W. J., Wu, F., and Yoden, S.: An
update of observed stratospheric temperature trends, Journal of Geophysical Research (Atmospheres), 114,
D02107, doi:10.1029/2008JD010421, 2009.

655 Revell, L. E., Bodeker, G. E., Huck, P. E., Williamson, B. E., and Rozanov, E.: The sensitivity of stratospheric
ozone changes through the 21st century to N_2O and CH_4, Atmospheric Chemistry & Physics, 12, 11 309–
11 317, doi:10.5194/acp-12-11309-2012, 2012.

Shepherd, T. G. and McLandress, C.: A robust mechanism for strengthening of the Brewer–Dobson circulation
in response to climate change: Critical-layer control of subtropical wave breaking, Journal of the Atmo-

660 spheric Sciences, 68, 784–797, 2011.

Shine, K. P., Bourqui, M., Forster, P. d. F., Hare, S., Langematz, U., Braesicke, P., Grewe, V., Ponater, M.,
Schnadt, C., Smith, C., et al.: A comparison of model-simulated trends in stratospheric temperatures, Quar-
terly Journal of the Royal Meteorological Society, 129, 1565–1588, 2003.

Smalley, K. M., Dessler, A. E., Bekki, S., Deushi, M., Marchand, M., Morgenstern, O., Plummer, D. A., Shi-

665 bata, K., Yamashita, Y., and Zeng, G.: Contribution of different processes to changes in tropical lower-
stratospheric water vapor in chemistry-climate models, Atmospheric Chemistry & Physics, 17, 8031–8044,
doi:10.5194/acp-17-8031-2017, 2017.

Sofieva, V., Kyrölä, E., Laine, M., Tamminen, J., Degenstein, D., Bourassa, A., Roth, C., Zawada, D., Weber, M., Rozanov, A., Rahpoe, N., Stiller, G., Laeng, A., von Clarmann, T., Walker, K., Sheese, P., Hubert, D.,
670   van Roozendael, M., Zehner, C., Damadeo, R., Zawodny, J., Kramarova, N., , and Bhartia, P.: Merged SAGE II, Ozone_cci and OMPS ozone profiles dataset and evaluation of ozone trends in the stratosphere, Atmos. Chem. Phys. Discuss., doi:10.5194/acp-2017-598, 2017.

Solomon, S., Ivy, D. J., Kinnison, D., Mills, M. J., Neely, R. R., and Schmidt, A.: Emergence of healing in the Antarctic ozone layer, Science, 353, 269–274, doi:10.1126/science.aae0061, 2016.

675 SPARC/WMO: SPARC Report on the Evaluation of Chemistry-Climate Models, SPARC, 2010.

Steinbrecht, W., Froidevaux, L., Fuller, R., Wang, R., Anderson, J., Roth, C., Bourassa, A., Degenstein, D., Damadeo, R., Zawodny, J., Frith, S., McPeters, R., Bhartia, P., Wild, J., Long, C., Davis, S., Rosenlof, K., Sofieva, V., Walker, K., Rahpoe, N., Rozanov, A., Weber, M., Laeng, A., von Clarmann, T., Stiller, G., Kramarova, N., Godin-Beekmann, S., Leblanc, T., Querel, R., Swart, D., Boyd, I., Hocke, K., Kämpfer,
680   N., Maillard Barras, E., Moreira, L., Nedoluha, G., Vigouroux, C., Blumenstock, T., Schneider, M., Garcìa, O., Jones, N., Mahieu, E., Smale, D., Kotkamp, M., Robinson, J., Petropavlovskikh, I., Harris, N., Hassler, B., Hubert, D., and Tummon, F.: An update on ozone profile trends for the period 2000 to 2016, Atmos. Chem. Phys. Discuss., 2017, 1–24, doi:10.5194/acp-2017-391, https://www.atmos-chem-phys-discuss.net/acp-2017-391/, 2017.

685 Stone, K. A., Solomon, S., and Kinnison, D. E.: On the Identification of Ozone Recovery, Geophys. Res. Lett., 45, 5158–5165, doi:10.1029/2018GL077955, 2018.

Thomason, L., Ernest, N., Millan, L., Rieger, L., Bourassa, A., Vernier, J., Peter, T., Luo, B., and Arfeuille, F.: A global, space-based stratospheric aerosol climatology: 1979 to 2016, Earth Syst. Sci. Data, in preparation, doi:10.5067/GloSSAC-L3-V1.0, 2017.

690 Tiao, G. C., Xu, D., Pedrick, J. H., Zhu, X., and Reinsel, G. C.: Effects of autocorrelation and temporal sampling schemes on estimates of trend and spatial correlation, Journal of Geophysical Research, 95, 20 507–20 517, doi:10.1029/JD095iD12p20507, 1990.

Wargan, K., Orbe, C., Pawson, S., Ziemke, J. R., Oman, L. D., Olsen, M. A., Coy, L., and Emma Knowland, K.: Recent Decline in Extratropical Lower Stratospheric Ozone Attributed to Circulation Changes, Geophys.
695   Res. Lett., 45, 5166–5176, doi:10.1029/2018GL077406, 2018.

Weber, M., Coldewey-Egbers, M., Fioletov, V. E., Frith, S. M., Wild, J. D., Burrows, J. P., Long, C. S., and Loyola, D.: Total ozone trends from 1979 to 2016 derived from five merged observational datasets - the emergence into ozone recovery, Atmospheric Chemistry & Physics, 18, 2097–2117, doi:10.5194/acp-18-2097-2018, 2018.

700 WMO: Scientific Assessment of Ozone Depletion: 2006, Global Ozone Research and Monitoring Project, 2006.

WMO: Scientific Assessment of Ozone Depletion: 2014 Global Ozone Research and Monitoring Project Report, World Meteorological Organization, p. 416, geneva, Switzerland, 2014.

WMO: Scientific Assessment of Ozone Depletion: 2018, Global Ozone Research and Monitoring Project–Report, World Meteorological Organization, p. 588, geneva, Switzerland, 2018.

705 Zerefos, C., Kapsomenakis, J., Eleftheratos, K., Tourpali, K., Petropavlovskikh, I., Hubert, D., Godin-Beekmann, S., Steinbrecht, W., Frith, S., Sofieva, V., and Hassler, B.: Representativeness of single lidar

stations for zonally averaged ozone profiles, their trends and attribution to proxies, Atmospheric Chemistry & Physics, 18, 6427–6440, doi:10.5194/acp-18-6427-2018, 2018.

Ziemke, J. R., Oman, L. D., Strode, S. A., Douglass, A. R., Olsen, M. A., McPeters, R. D., Bhartia, P. K., Froide-
710   vaux, L., Labow, G. J., Witte, J. C., Thompson, A. M., Haffner, D. P., Kramarova, N. A., Frith, S. M., Huang, L.-K., Jaross, G. R., Seftor, C. J., Deland, M. T., and Taylor, S. L.: Trends in Global Tropospheric Ozone Inferred from a Composite Record of TOMS/OMI/MLS/OMPS Satellite Measurements and the MERRA-2 GMI Simulation, Atmospheric Chemistry and Physics Discussions, 2018, 1–29, doi:10.5194/acp-2018-716, https://www.atmos-chem-phys-discuss.net/acp-2018-716/, 2018.